The right ventricle under pressure: evaluating the adaptive and maladaptive changes in the right ventricle in pulmonary arterial hypertension using echocardiography (2013 Grover Conference series)

Alexis Harrison,[1] Nathan Hatton,[2] John J. Ryan[1]

[1]Division of Cardiovascular Medicine, Department of Medicine, University of Utah, Salt Lake City, Utah, USA; [2]Division of Pulmonary Medicine, Department of Medicine, University of Utah, Salt Lake City, Utah, USA

Abstract: The importance of the right ventricle (RV) in pulmonary arterial hypertension (PAH) has been gaining increased recognition. This has included a reconceptualization of the RV as part of an RV–pulmonary circulation interrelated unit and the observation that RV function is a major determinant of prognosis in PAH. Noninvasive imaging of RV size and function is critical to the longitudinal management of patients with PAH, and continued understanding of the pathophysiology of pulmonary vascular disease relies on the response of the RV to pulmonary vascular remodeling. Echocardiography, in particular the newer echocardiographic measurements and techniques, allows easy, readily accessible means to assess and follow RV size and function.

Keywords: imaging, three-dimensional echocardiography, tricuspid annular plane systolic excursion, right heart failure, right ventricular function.

Pulm Circ 2015;5(1):29-47. DOI: 10.1086/679699.

Pulmonary arterial hypertension (PAH) is characterized by severe remodeling of distal pulmonary arterioles due to a complex interplay between genetic and molecular factors.[1,2] This remodeling is characterized by intimal hyperplasia, vasoconstriction, medial hypertrophy, and the development of plexiform lesions, all of which contribute to and result in higher pulmonary artery pressure. The prevalence of PAH is 7–15 individuals per million people.[3,4] A diagnosis of PAH is initially suggested by symptoms including dyspnea, syncope, and exertional intolerance and is usually evaluated first with echocardiography.[5] Echocardiography may suggest elevated pulmonary artery pressures (PAPs) and help formulate a working hypothesis regarding the etiology of the presumed pulmonary hypertension (PH), but right heart catheterization remains essential to provide final hemodynamic classification of PH and, with that knowledge in hand, to guide appropriate World Health Organization (WHO) PH group–specific therapy.[6] Once the diagnosis of PAH is established (mean PAP $\geq$ 25 mmHg and pulmonary capillary wedge pressure $\leq$ 15 mmHg), most clinicians rely on a combination of frequent clinical evaluations and echocardiography to follow therapeutic response and to give insight into the effects of elevated PAP on the structure and function of the right ventricle (RV). The right ventricle's adaptation or maladaptation to the increased afterload is often a sign of the severity of PH.[7]

The relevance of the relationship between the RV and the pulmonary circulation in PAH has been gaining increased recognition.[8] As a pump, the RV generates the same stroke volume as the left ventricle (LV) with one-fourth the stroke work because of the lower resistance of the normal pulmonary vasculature.[9] The RV is thin walled, with the free wall measuring 2–5 mm, and contains one-sixth the muscle mass of the LV.[9] It is a crescent-shaped chamber with a high capacitance and a greater ability to handle changes in preload than in afterload. When chronically exposed to increased afterload, the RV can adapt with myocardial hypertrophy, since increase in wall pressure leads to increase in wall stress that, by way of LaPlace's law, can be tempered by increased wall thickness. However, maladaptive changes can subsequently occur that lead to

Address correspondence to Dr. John Ryan, FAHA, FACC, University Hospital Cardiovascular Center, 50 N Medical Drive, Salt Lake City, UT 84132, USA. E-mail: john.ryan@hsc.utah.edu.

Submitted July 9, 2014; Accepted August 19, 2014; Electronically published February 20, 2015.

RV dilation and a decreased contractility.[7] Concomitant with the pressure burden, metabolic shifts, neurohormonal signal alterations, ischemia, oxidative stress, and inflammation have been proposed to adversely affect the RV in PAH and may play a role in the development of RV dysfunction.[10] Ultimately, RV remodeling and RV dysfunction have been associated with a poor prognosis, and RV failure is a leading cause of death in PAH.[10,11]

With the advances made in echocardiographic techniques, in particular 3-dimensional (3D) echocardiography and speckle-tracking right ventricular (RV) strain, RV imaging by transthoracic echocardiography (TTE) has improved considerably, enabling the acquisition of accurate assessment of RV function. Echocardiography is also more affordable for serial testing and more universally available than more advanced cardiac imaging tests such as cardiac magnetic resonance imaging (MRI) and positron emission tomography. In this review of using echocardiography to follow the RV in the setting of PAH, we outline the ability of Doppler, 2-dimensional (2D), and 3D echocardiography to assess RV structure and function, and we propose that echocardiography will remain the mainstay in the evaluation of the RV in PAH throughout patient management in developed and developing countries.

THE ROLE OF ECHOCARDIOGRAPHY IN THE DIAGNOSIS OF PAH

Doppler echocardiography represents the most accessible screening tool for PAH[12-14] with an estimation of the RV systolic pressure (RVSP). The RVSP is calculated from Bernoulli's principle on the basis of the velocity of the tricuspid regurgitant (TR) jet ($4v^2$, where v is the maximum velocity of the tricuspid valve regurgitant jet, plus the estimated right atrial [RA] pressure). Recognizing that the RVSP measurement is only an estimate and subject to error,[15] the measurement should be interpreted in context of the information on the echocardiogram as a whole. In a meta-analysis, Janda and colleagues[16] showed only modest sensitivity and specificity for the use of peak TR jet velocities to estimate the RVSP, in combination with RA pressures, to diagnose PH (sensitivity of 83% and specificity of 72%). In addition, Rich and colleagues[15] have shown the tendency for misclassification of pressures by TR jet velocity with both underestimation and overestimation of pulmonary artery systolic pressures.

On the other hand, even when the estimated RVSP is normal, other echocardiographic parameters may suggest RV dysfunction, which ultimately may be related to undiagnosed PAH (Table 1). No significant tricuspid regurgita-

Table 1. Right ventricular structural echocardiography parameters

Parameter	Echo view	Normal value
2D RV measurements		
RV basal diameter, mm	RV focused apical 4CH	<41
RV midcavity diameter, mm	RV focused apical 4CH	<35
RV base-apex RV longitudinal diameter, mm	RV focused apical 4CH	≤83
Indexed RV end-diastolic area in men, cm^2/m^2	RV focused apical 4CH	≤12.6
Indexed RV end-diastolic area in women, cm^2/m^2	RV focused apical 4CH	≤11.5
RVOT proximal, mm	Parasternal short axis	≤35
RVOT distal, mm	Parasternal short axis	≤27
RVOT wall thickness, mm	Parasternal long or subcostal	≤5
3D RV measurements		
Indexed RV end-diastolic volume in men, mL/m^2		≤87
Indexed RV end-diastolic volume in women, mL/m^2		≤74
RV EF, %		≥45
2D RA dimensions		
Indexed RA volume in men, mL/m^2	Apical 4CH	25 ± 7
Indexed RA volume in women, mL/m^2	Apical 4CH	21 ± 6

Note: EF: ejection fraction; RA: right atrial; RV: right ventricular; RVOT: RV outflow tract; 2D: 2-dimensional; 3D: 3-dimensional; 4CH: 4-chamber. The 2D RV normal values, 2D RA normal values, and 3D normal volumes are from American Society of Echocardiography guidelines.[33]

tion (TR) or low/normal estimated RVSP has been noted in 10%–25% of patients with PH, as the TR Doppler profile may be insufficient to measure.[6,17] Thus, specific evaluation for evidence of RV dysfunction is of paramount importance if there is clinical suspicion of PH and should prompt the clinician to pursue further clinical workup.

THE RELATIONSHIP BETWEEN THE RV AND PROGNOSIS IN PAH

Many echocardiographic RV parameters have been shown to be key determinants in the prognosis in PAH[10] as the RV adapts to the elevated pulmonary vascular resistance (PVR), with poor adaptation significantly contributing to mortality.[18,19] Parameters that have correlated with an increased mortality risk in PAH include evidence of right-sided pressure overload with secondary abnormal RV systolic and diastolic function, the presence of pericardial effusion, increased RA area indexed to height, increased RV diameter, decreased tricuspid annular plane systolic excursion (TAPSE), decreased Tei index, alterations in RV free-wall strain, and decreased isovolumic contraction velocity (IVCv).[20-29] These are reflective of increasing RV and RA size and decreased RV contractility. A thorough discussion of how to obtain these parameters and the limitations of each one are outlined below.

Interestingly, the presence of a mild-to-moderate pericardial effusion has also long been associated with chronic severe PAH[30] and has consistently been shown to correlate with increased mortality.[20-23] The development of a pericardial effusion in PAH is proposed to be the result of high RA pressures from RV dysfunction. This subsequently inhibits lymphatic drainage via the thoracic duct and may increase in proportion to the elevated RA pressure.

ASSESSMENT OF RV STRUCTURE

The differences between the RV and the LV include structural, embryological, genetic, and neurohormonal responses.[9,31,32] Structurally, the healthy RV is an anterior, thin-walled, trabeculated, crescent-shaped structure with a complex geometry that wraps around the ellipsoid LV and has been delineated anatomically into the inlet, the trabeculated apex, and the infundibulum. The RV contracts in a peristolic ("bellows") motion,[9] which is the result of contraction from predominantly longitudinal muscle fibers. The structure and orientation of the RV in the anterior chest, as well as its unique shape, have made it challenging to fully characterize the RV by 2D echocardiography. The RV sits close to the anterior chest wall and may be subject to poorer near-field resolution, and there is no one echocardiographic view that is able to completely visualize the whole of the RV. Thus, different probe orientations are used to assess the RV in piecemeal fashion, including the parasternal long- and short-axis views, the RV inflow view, the apical 4-chamber view, and the subcostal views (Fig. 1).[33]

Figure 1 summarizes the segmental anatomy of the RV in different echocardiographic views.[34] To assess RV size and volume, the American Society of Echocardiography proposes the use of standard 2D size measurements from parasternal short-axis and apical 4-chamber views of the heart (Figs. 2, 3).[33] However, these measurements correlate poorly with 3D volumes obtained with echocardiography and are highly dependent on probe and patient positions[35,36] and therefore have been the subject of criticism of the true assessment of RV size.[37] Use of 2D methods, such as Simpson's method of disks, underestimates volumes of the RV because of the crescentic shape of the RV.[38] The size and shape of the RV are also intrinsically linked to those of the LV, and visual estimation of RV size is often made relative to that of the LV.[8] However, qualitative measurements of the RV size and function have wide interobserver variability, compared with quantitative assessment.[39]

Over time in PAH, with the associated chronic afterload elevation, the RV dilates. This is noted when an end-diastolic RV area approximates or is greater than that of

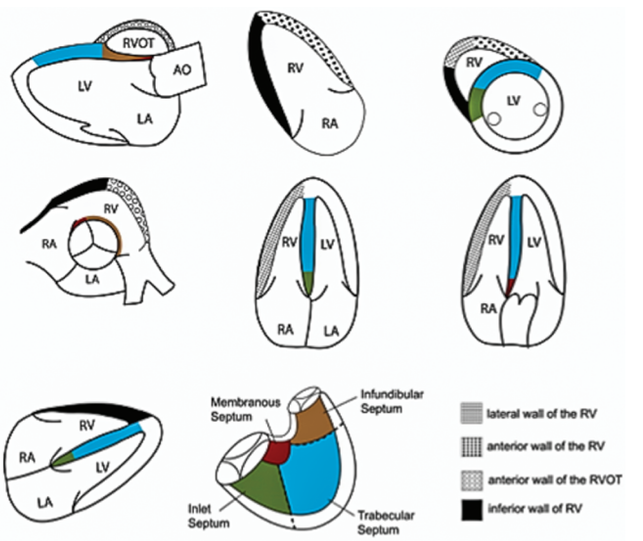

Figure 1. Segmental anatomy of the right ventricle (RV), as shown in representative echocardiographic views. The colors indicate the different subdivisions of the interventricular septum. AO: aorta; LA: left atrium; LV: left ventricle; RA: right atrium; RVOT: right ventricular outflow tract. Adapted from Jiang[34] with permission from the publisher (copyright 1994, Lippincott Williams & Wilkins).

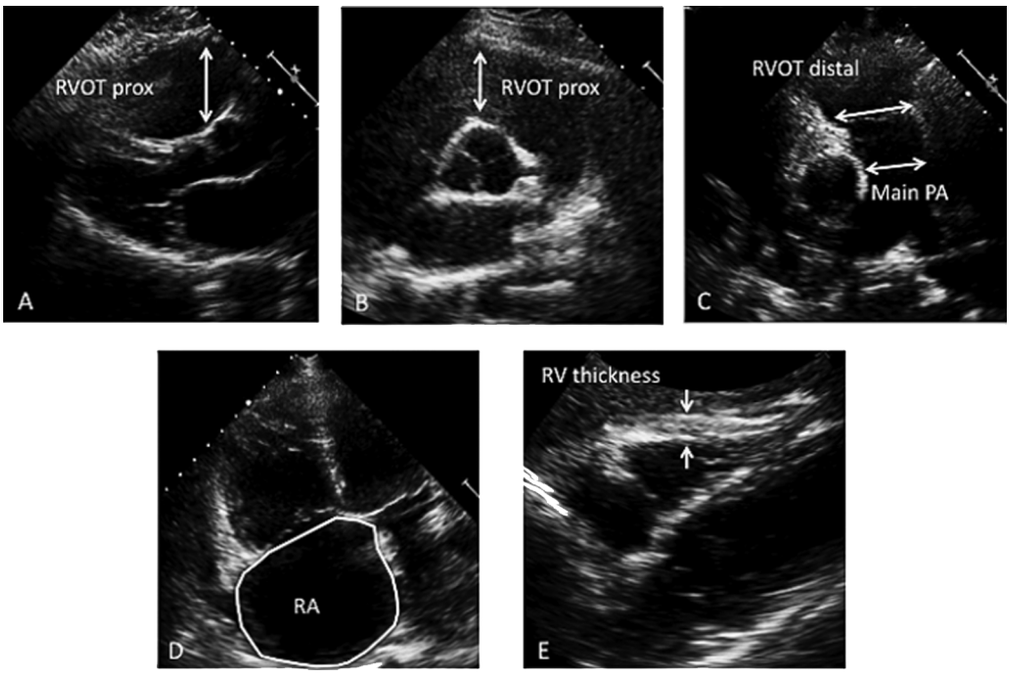

Figure 2. Examples of 2-dimensional echocardiographic chamber dimensions and RV wall thickness. *A*, Parasternal long-axis view and the proximal RVOT diameter. *B*, Basal parasternal short-axis view and the proximal RVOT diameter. *C*, Parasternal short-axis view of the pulmonary bifurcation and the main PA measurement. The RVOT distal measurement is made in this view just above the pulmonary valve. *D*, Right atrial volume in the apical 4-chamber view in end-systole when the RA has the largest area. *E*, RV wall thickness, measured in the subcostal view at end-diastole. PA: pulmonary artery; RA: right atrium; RV: right ventricular; RVOT: RV outflow tract.

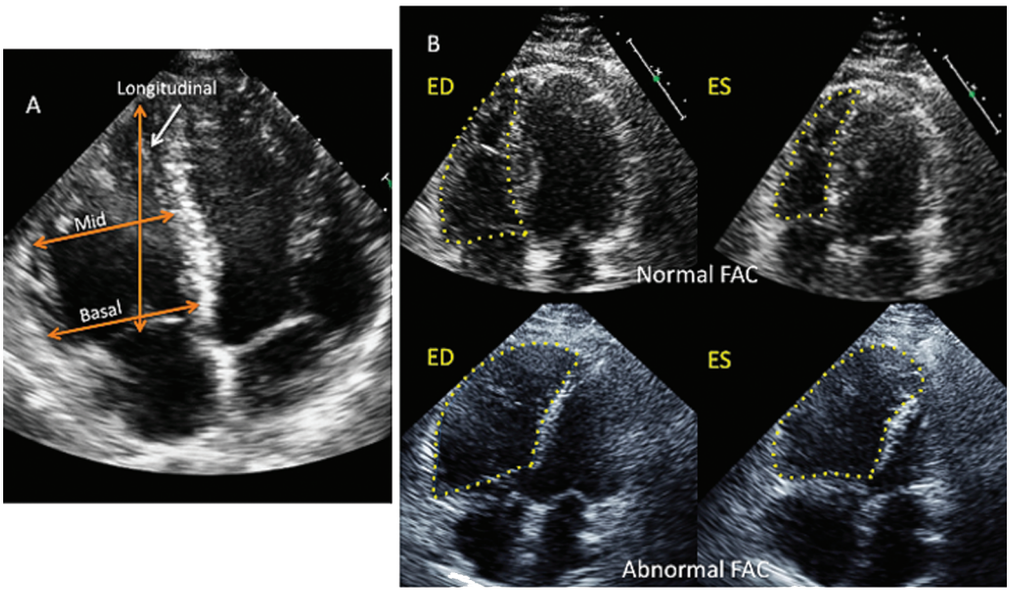

Figure 3. RV dimension and area measurements in the apical 4-chamber view. *A*, Basal, midcavity, and longitudinal RV dimensions. *B*, The upper panel shows an RV with normal systolic function and a normal FAC. The lower panel shows a markedly dilated RV with decreased function and an abnormal FAC. The calculation of percentage FAC is [(area at ED − area at ES)/area at ED)] × 100. ED: end-diastole; ES: end-systole; FAC: fractional area change; RV: right ventricle.

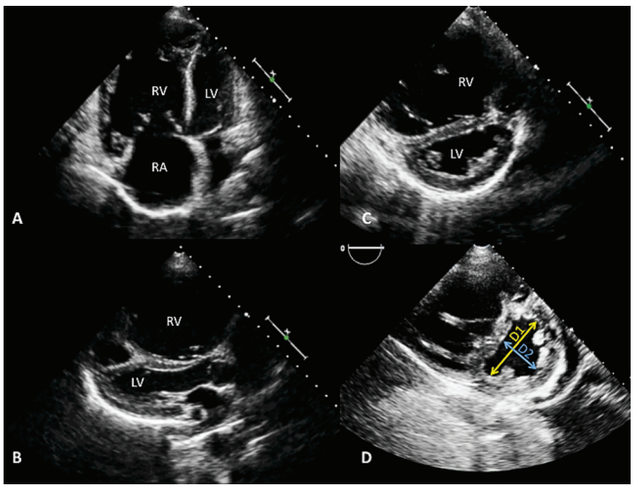

Figure 4. Two-dimensional echocardiography of RV and LV size and ventricular interdependence. *A*, Apical 4-chamber view showing an enlarged RV, where the RV is larger than the LV. *B*, Parasternal long-axis view with an enlarged RV and bowing of the septum into the LV chamber. *C*, Flattening of the ventricular septum, forming a D-shaped short-axis LV appearance. *D*, Representation of the end-diastolic eccentricity index, which is the ratio between the LV anteroposterior dimension (D1) and LV septolateral dimension (D2). LV: left ventricle; RA: right atrium; RV: right ventricle.

the LV in the apical 4-chamber view (Fig. 4*A*, 4*B*). Ghio and colleagues[26] showed that patients with an RV end-diastolic diameter greater than 36.5 mm, measured on the parasternal long-axis view, had a higher mortality than patients with an RV end-diastolic diameter of up to 36.5 mm, with a hazard ratio of 2.64. Similarly, increased RA area indexed to height, a reflection of high atrial pressures, has been shown to predict increased mortality.[20,40]

RV WALL THICKNESS

Chronic RV pressure overload seen in PAH can induce RV hypertrophy (RVH), which is an adaptive change to the increased afterload. The increased RV thickness is a reflection of an increase in total RV mass. Using subcostal views of the RV, an end-diastolic free-wall thickness greater than 5 mm indicates hypertrophy and remodeling in response to chronically elevated afterload.[41] No studies have shown survival benefit or hazard with increased RV hypertrophy in PAH. Ghio and colleagues[42] looked at RV wall thickness in a small study of 59 patients with severe PH (mean PAP = 54 mmHg and PVR = 14 Wood units) from idiopathic PAH, followed these patients for an average of 52 months, and found that the mean RV free-wall thickness in this group was 3.8 mm. Although in the general population and in heart failure with preserved ejection fraction (EF), RVH has been found to be predictive of worse outcomes,[43,44] in idiopathic PAH there was no significant association with survival or mortality based on wall thickness. However, the finding of normal wall thickness in severe PAH suggests that there may be a predominance of maladaptive RV remodeling or a mix of adaptive and maladaptive remodeling responses.[12]

ABNORMAL INTERVENTRICULAR WALL MOTION AS A SIGN OF VENTRICULAR INTERDEPENDENCE

Despite the differences between the LV and the RV, their functions are not independent of each other.[45] The RV has a critically important anatomic and physiologic interdependence with the LV that must be understood to appreciate the effects of RV dysfunction and failure. Anatomically, the RV shares the septum with the LV, with attachments at the anterior and posterior septum; has mutually encircling epicardial fibers; and is jointly enclosed within the intrapericardial space.[35] This interdependence is evident in many cardiac disease processes, including restrictive and constrictive pathophysiology.[46] With RV pressure or volume overload, a bowing and flattening of the interventricular septum (IVS) toward the LV is noted (Fig. 4*C*; Video 1, available online). A greater degree of septal shift occurs toward end-systole in chronic pressure overload. RV volume overload may also result in septal flattening and shifting of the IVS, predominantly during diastole and especially toward end-diastole. This leftward bowing of the IVS contributes to decreased LV filling and a reduc-

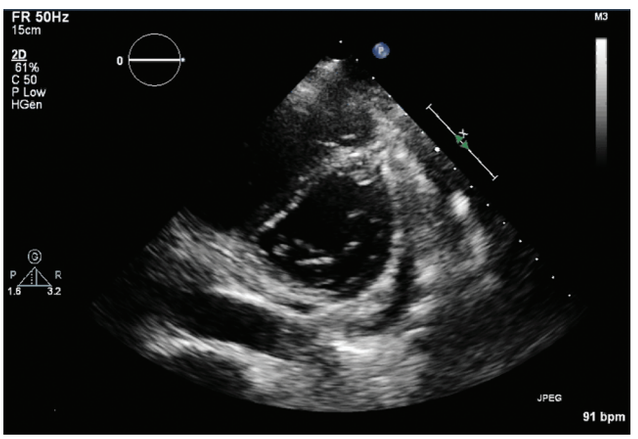

Video 1. Image from a video, available online, showing an example of severe right ventricular volume and pressure overload with flattening of the interventricular septum throughout the cardiac cycle.

tion in stroke volume. The ratio of the end-diastolic anteroposterior distance to the septal-lateral distance on short-axis views of the LV at end-diastole is referred to as the LV eccentricity index, and a ratio greater than 1 is indicative of RV overload (Fig. 4*D*).[47] Physiologically, with RV dilation and a septum shift leftward, the RV loses the normal LV septal contractile force's contribution to RV stroke work, amounting to approximately one-third of the work. This septal flattening may in turn negatively affect LV filling and RV perfusion from decreased peak LV pressures.[9]

RV FUNCTION

As discussed above, survival in PAH and the severity of symptoms are strongly associated with RV function.[48] Historically, since the RV has been so difficult to visualize by 2D echocardiography, numerous ways were developed to assess RV function (Table 2). The traditional surrogate measures of RV performance are fractional area change (FAC), which is defined as [(RV end-diastolic area − RV end-systolic area)/RV end-diastolic area] × 100 and measured in the apical 4-chamber view; TAPSE, which is the M-mode measurement of the longitudinal displacement of the tricuspid annulus; and RV myocardial performance index (RV-MPI), which is the ratio of total isovolumic time to ejection time. Newer 2D echocardiographic methods to quantify RV function include the RV free-wall longitudinal systolic tissue velocity (*S*′), measured with pulse-wave or color Doppler tissue imaging (DTI); the first derivative of RV pressure (dP/dt_{max}); IVCv; and RV strain imaging.

The measurement of RV FAC is demonstrated in Figure 3. A good correlation has been observed between RV FAC and RVEF, and it appears to be the 2D measure of RV function that best correlates with RV systolic function measured on cardiac MRI.[49,50]

TAPSE assesses longitudinal RV function through the use of the M-mode in the apical 4-chamber view (Fig. 5*A*). A focus on quantitative measures of RV function has centered on estimating the longitudinal shortening, or base-to-apex movement, of the RV, since this motion has been presumed to contribute more to the RV stroke volume than circumferential shortening.[51] TAPSE has been shown to be a reliable predictor of prognosis in PAH and a measure of RV function, with a value of less than 18 mm predicting mortality from PAH.[25] Acquisition of TAPSE is angle dependent and preload and afterload dependent. Some concern has been raised about the accuracy of TAPSE when compared with EFs obtained with cardiac MRI, as TAPSE represents only basal RV systolic function and therefore is not reflective of global function as well as being influenced by passive translational or tethering forces.[50]

Forfia and colleagues[25] evaluated TAPSE in a prospective study of 63 patients with PAH. Patients with TAPSE no greater than 1.8 cm had a survival estimate of 50% at 2 years, compared with 88% 2-year survival in patients with TAPSE greater than 1.8 cm.[25] In all, TAPSE is likely the most widely used and reproducible technique to follow RV function, although the timing of the deterioration in TAPSE relative to the onset of RV failure is ill defined.[52]

The RV-MPI, also known as the Tei index, incorporates elements of both systolic and diastolic phases in the assessment of global ventricular function (Fig. 5*B*). The Tei index is defined as the sum of the isovolumic contraction and the isovolumic relaxation times divided by ejection time.[53] These measurements can be obtained on either DTI of the tricuspid annulus or pulsed-wave Doppler imaging of the RV outflow for the ejection time and from either tricuspid valve inflow or regurgitation for the tricuspid valve opening time. Values greater than 0.55 by DTI and greater than 0.40 by pulsed-wave Doppler reflect RV dysfunction.[37] The Tei index correlates well with RVEF[54] and is less affected by heart rate or loading conditions, thereby making it more reproducible. In a series of 53 patients studied by Yeo and colleagues,[24] a Tei index cut-off value of at least 0.83 was associated with decreased 1-, 2-, and 5-year survival of 71%, 28%, and 4%, respectively, compared to a Tei index of less than 0.83, which had 1-, 2-, and 5-year survival of 96%, 87%, and 73%, respectively.

Pulsed DTI of the tricuspid annulus records the peak systolic tricuspid lateral annular velocity (*S*′; Fig. 5*C*), which is a reflection of systolic longitudinal RV myocardial contractility. An *S*′ of less than 9.7 cm/s is associated with abnormal RV contractility, and *S*′ has been shown to be potentially useful in the early detection of RV dysfunction.[12,55] The *S*′ is inversely related to PVR and correlates with RVEF.[56] Acquisition is limited by angle dependence and tethering effects, similar to TAPSE, as this measurement is taken at the same angle and is focused on the same lateral segment of the tricuspid annulus as TAPSE.

The dP/dt_{max} as the RV pressure changes by 12–15 mmHg (depending on the measurement of velocities from 1 to 2 m/s or from 0.5 to 2 m/s) is a useful measure in the assessment of RV systolic function and contractility (Fig. 5*D*).[57] This index can be noninvasively estimated by continuous-wave Doppler echocardiography using TR.[58] However, the Doppler-derived dP/dt_{max} has not been used routinely as a clinical index because it depends on preload and is sensitive to the incident angle. The dP/dt_{max} is independent of afterload. Some investigators contend that

Table 2. Right ventricle functional echocardiography parameters, prognostic significance

Parameter	Echo view	Normal value[a]	Prognosis	Limitation
RV FAC,[b] %	Apical 4CH	>35		Difficult endocardial delineation due to trabeculations; delineation of anterior wall; identification of infundibular plane; load dependent
TAPSE, mm (Fig. 5*A*)	Apical 4CH M-mode of lateral tricuspid annulus	≥17	TAPSE < 18 associated with increased RV dysfunction, increased 1- and 2-year mortality and hazard ratio of 5.7[25]	Load dependent; angle dependent; cannot use if tricuspid annuloplasty; assesses only RV inflow
dP/dt_{max}, mmHg/s	Apical 4CH pulse Doppler TR	<400		Preload dependent; angle dependent; not as reliable in significant TR
Tei index, or MPI[c]	Apical 4CH pulse Doppler TR or DTI of lateral tricuspid annulus	Doppler: ≤0.43; DTI: ≤0.54	MPI of <0.83 had a 5-year survival free of death or lung transplantation of 74%, compared to 4% for MPI ≥ 0.83, with a hazard ratio of 1.3 for every 0.1 unit increase[24]	Less affected by load dependence and heart rate; arrhythmia sensitive in the pulse-wave Doppler method; may be underestimated in high RAPs (as IVRT decreases)
DTI *S′*, cm/s (Fig. 5*C*)	Apical 4CH DTI of lateral tricuspid annulus	≥9.5		Angle dependent; less load dependent; can calculate MPI at the same time
IVA, m/s^2	Apical 4CH DTI of lateral tricuspid annulus	1.4–3.0		Angle dependent; HR dependent; low reproducibility
IVCv, cm/s	Apical 4CH DTI of the lateral tricuspid annulus	≥9	Independent predictor of mortality with 1-year survival of 95% if IVCv > 9 and 80% if IVCv ≤ 9; hazard ratio: 3.68[28]	Angle dependent
RV diastolic function	Apical 4CH Doppler of RV inflow at tips of tricuspid valve	*E*/*e′* > 6 predicts RAP > 10 mmHg; *E*/*A* < 0.8: impaired relaxation; *E*/*A* = 0.8–2.0 and diastolic predominance in hepatic veins: pseudonormal filling; *E*/*A* > 2.0 and DT < 119: restrictive filling		Angle dependent; load dependent; not well studied in severe TR;arrhythmia sensitive; expected to show small *E*/*A* decrease with increasing age
Strain imaging	Speckle-tracking strain		RV free-wall strain of <−12.5% was associated with decreased 1 year survival (61%, vs. 89% if strain > −12.5%);[27] RV strain predicted outcome with a 1.46 higher risk of death (95% CI: 1.05–2.12) for every 6.7% decline in strain[66]	Requires additional processing; vendor specific

Note: *A*: tricuspid peak A-wave velocity; CI: confidence interval; DTI: Doppler tissue imaging; *E*: tricuspid peak E-wave velocity; *e′*: tricuspid early myocardial velocity; ET: ejection time; FAC: fractional area change; IVA: isovolumic acceleration; IVCv: isovolumic contraction velocity; IVCT: isovolumic contraction time; IVRT: isovolumic relaxation time; MPI: myocardial performance index; RAP: right atrial pressure; RV: right ventricle; *S′*: systolic velocity; TAPSE: tricuspid annular plane systolic excursion; TR: tricuspid regurgitation; 4CH: 4-chamber view.

[a] Based on Lang et al.[33]

[b] [(End-diastolic area − end-systolic area)/end-diastolic area] × 100.

[c] (IVRT + IVCT)/(RV ET); Figure 5*B*.

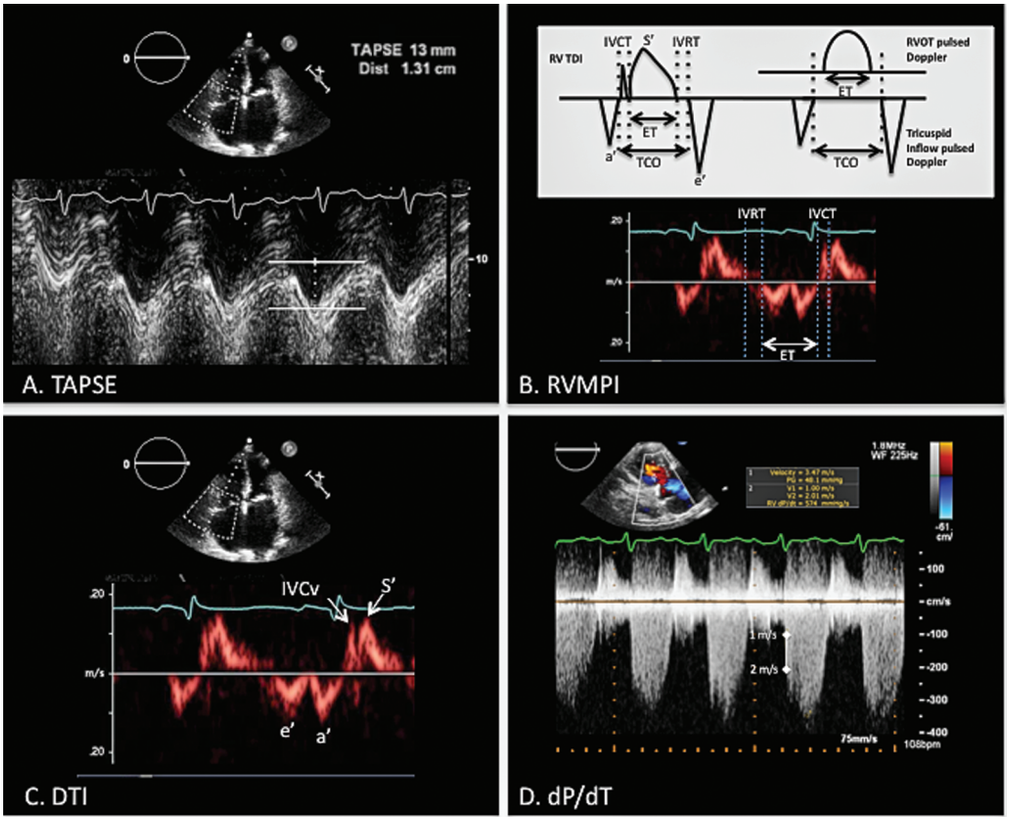

Figure 5. Surrogate echocardiographic markers of right ventricle (RV) function. *A*, Tricuspid annulus plane systolic excursion (TAPSE). M-mode cursor placed through the RV apex to the lateral tricuspid annulus in the apical 4-chamber view for the purpose of measuring the distance traveled by the annulus in centimeters from end-diastole to end-systole. Abnormal TAPSE of 1.3 cm is noted by cross-hatching. *B*, RVMPI (Tei index). *Top*, representation of the two ways to calculate RVMPI: on tissue Doppler and on pulsed-wave Doppler. *Bottom*, isovolumic contraction and relaxation times (IVCT and IVRT, respectively) and ejection time (ET), where right ventricular myocardial performance index (RVMPI) = (IVCT + IVRT)/ET. *C*, Doppler tissue imaging (DTI) of the tricuspid annulus after pulsed-wave interrogation of the lateral wall of the tricuspid annulus. These measurements can be made after high-frame-rate acquisition with color-coded Doppler offline (not shown). IVCv: isovolumic contraction velocity; *S'*: highest systolic velocity. *D*: Rate of pressure rise in the RV, or the dP/dT. On the ascending limb of the continuous Doppler image of the tricuspid regurgitation jet, the time for the velocity to increase from 1 to 2 m/s is measured, and the dP/dT is 12 mmHg/time in seconds.

dividing the derivative of the RV pressure by the maximum pressure (dP/dt_{max}) is a more accurate measure of RV contractility because it does not have the load- and angle-dependent features.[59]

The IVCv is the peak velocity by DTI measurement at the level of the tricuspid annulus that is taken during isovolumic contraction, a period in the cardiac cycle in early systole when the RV contracts and pressures rise acutely without any change in ventricular volume (a brief period after the tricuspid valve is closed and before the pulmonic valve is open). It is the velocity deflection seen just before the *S'* deflection on DTI. This contractility is relatively preload and afterload independent and may reflect a more global ventricular contractility.[60] Ernande and colleagues[28] found IVCv to be an independent predictor of mortality in PAH by multivariate analysis, with a 1-year survival of 95% if IVCv exceeds 9 cm/s and 80% if it does not, with an associated hazard ratio of 3.68.

FUTURE DIRECTIONS OF RV ASSESSMENT

As acquisition of RV physiology improves and our understanding of RV function changes, the aforementioned descriptions of RV function may become obsolete. Looking at the movement of one side of the tricuspid annulus and measuring DTI from this region may not be as valuable once RV strain and 3D RVEF become more advanced and adopted.[61] However, many echocardiographic laboratories are currently using the conventional measures along with

the newer methods described below for complete RV echocardiographic analysis.[62]

RV STRAIN

Advances in echocardiographic evaluation of the RV have improved the ability to assess RV strain. Strain is a measurement of tissue deformation as the myocardium contracts in systole as a result of sarcomere shortening. The myocardial tissue deforms as the myocardial tissue changes 3D shape, with longitudinal shortening, circumferential shortening, and radial thickening. This deformation results in a smaller RV cavity and forward ejection of blood from the ventricle. We describe this myocardial deformation as strain, the percent change from the initial length in end-diastole or onset of the cardiac cycle.[63] Longitudinal shortening resulting in a negative strain can be measured with DTI in the apical 4-chamber view, and circumferential shortening strain, which is also a negative strain, is obtained in the short-axis view but is less standardized than longitudinal strain in the acquisition methods. Color DTI strain is limited by different ranges of "normal" provided by different echocardiogram vendors and is dependent on complex postprocessing, image acquisition, frame rate, and angle of acquisition.

Speckle tracking is a technique where the unique speckled back-scatter of the reflected ultrasound beam in the myocardium is followed frame by frame.[63] This is a more reliable measure of RV strain than DTI[64] and uses algorithms that identify and follow speckles in the myocardium on sequential frames, and strain values are derived from this movement. Unlike color DTI, speckle tracking is angle dependent, but it is dependent on image quality and frame rate. This method also allows for short-axis and long-axis strain measurement reliably.[64] The normal and abnormal values still vary, depending on the vendor providing the strain software, which makes comparison between centers very difficult.[61]

Worsening of RV longitudinal strain has been associated with increased pulmonary artery pressures, decreased TAPSE, worsened functional class, and increased mortality from PAH (Fig. 6).[65,66] RV strain has been shown to improve with vasodilator therapy,[67] and an improvement in

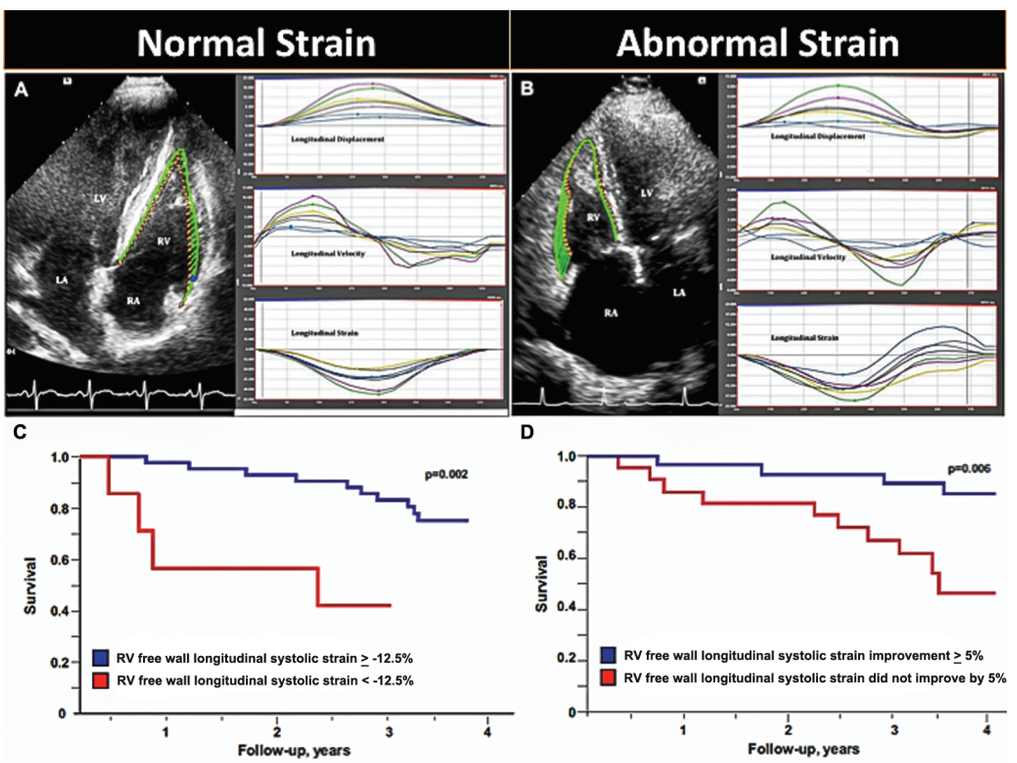

Figure 6. *A, B,* Velocity vector imaging showing normal (*A*) and abnormal (*B*) segmental patterns of longitudinal displacement, velocity, and strain. LA: left atrium; LV: left ventricle; RA: right atrium; RV: right ventricle. Adapted from Sanz et al.[37] with permission. *C,* A severe reduction in RV free-wall systolic strain at follow-up (<−12.5%) was associated with a poor prognosis over 4 years of subsequent follow-up ($P = 0.002$). *D,* An improvement in RV free-wall systolic strain by 5% was associated with a better survival over 4 years of follow-up ($P = 0.006$). *C* and *D* are adapted from Hardegree et al.[68] with permission.

strain in response to therapy is predictive of a favorable prognosis.[68]

3D ECHOCARDIOGRAPHIC ASSESSMENT OF THE RV

Although RVEF is highly dependent on loading conditions, it remains the most commonly used index of RV contractility. Under normal conditions, RVEF is lower than LVEF, because the RV chamber is larger than the LV chamber, with a normal range of RVEF varying between 40% and 76%, depending on the technique used.[69] A decline in RVEF is predictive of mortality and correlates with worsening functional class.[70,71]

RV volumes acquired with 3D TTE correlate considerably better than 2D TTE with the reference standard of cardiovascular MRI, but in the past this has been limited by suboptimal image quality.[72] In patients with dilated RV, the exclusion of the free wall from the imaging sector can lead to inaccuracy of RV volumes. Improvements in image acquisition technology are making this less prevalent and have overcome many of the difficulties surrounding 3D reconstruction of the RV. Currently, in order to acquire 3D volumes of the RV, tracings of anatomical landmarks are made at the end of diastole, and then, akin to speckle tracking, these sites are followed over the course of systole in order to reconstruct the 3D images. There remains a need to obtain 3–6 cardiac cycles to create full-volume imaging, and therefore this can be subject to increased error in the setting of arrhythmia. However, this method does facilitate imaging of the entire RV and can therefore measure RV volumes. These volume acquisitions and subsequent RVEF measurements have been validated compared to in vivo volumes and function, have demonstrated minimal interobserver variability (~4%), and have been found to be accurate and reproducible (Fig. 7*A*–7*C*).[73-75] Changes in RV function and volume based on 3D TTE correlate with symptoms in patients with PAH. Interestingly, Leary and colleagues[75] observed that RVEF obtained with 3D TTE did not correlate well with TAPSE. This likely reflects a limitation of TAPSE due to other influences on this parameter, such as LV function and respiration.

The technique of knowledge-based reconstruction has been applied to PAH in 3D echocardiography with some success. In the published versions of knowledge-based reconstruction in PAH, the technique involves the acquisition of 2D images localized in 3D space by a magnetic-field generator. A magnetic-field sensor is attached to the echocardiographic transducer, and the specific anatomic landmarks are identified and recorded by the user. A reconstruction algorithm uses these landmarks to generate a 3D model by cataloging them against patients with similar pathologies (Fig. 7*D*, 7*E*).[76] The generation of a 3D RV model from 2D transthoracic echocardiographic has been validated in vitro and against cardiac MRI in patients with congenital heart disease.[77,78] The RV end-diastolic volumes and RVEF in patients with PAH obtained through this technique correlate well with those seen in CMR.[79]

ECHOCARDIOGRAPHY AND RV HEMODYNAMICS

To understand how and why the RV adapts to the changes in the pulmonary circulatory system, one should take a thoughtful look at RV hemodynamics, including the afterload (PVR), preload (central venous pressure [CVP]), and contractility, as assessed in invasive RV pressure-volume loops or conceptualized in a calculated RV stroke-work index.[80] Just as worsening echocardiographic parameters of RV function have correlated with a worse prognosis, so have worsening cardiac hemodynamics indicative of the struggling RV (RA pressure >15 mmHg and cardiac index < 2.0 L/min/m^2).[81]

Doppler echocardiography can estimate the afterload and preload of the RV and can help clinicians understand the hemodynamic significance of any RV dysfunction.[82] The estimation of CVP can be made by assessing the size and collapsibility of the inferior vena cava (IVC) proximal to the hepatic veins.[83] An IVC that has a size greater than 2.1 cm and is also not collapsible by more than 50% suggests an RA pressure higher than 15 mmHg (range: 10–20 mmHg).[84,85] The collapsibility, or "sniff test," is assessed on inspiration because the intrapleural pressure drop leads to an increase in central venous return, a decrease in CVP, and an IVC that should collapse. The caveat is that young patients may have dilated IVCs at baseline and that assessment of high RA pressures cannot be made on positive pressure ventilation, although a collapsible IVC is indicative of low RA pressure on positive pressure ventilation. Afterload is most commonly evaluated as PVR, with PVR = (mean PAP − pulmonary capillary wedge pressure)/cardiac output.[86]

Other measures of the right-sided pressures estimated by Doppler echocardiography are noted in Table 3. Despite the advances in the assessment of right-sided hemodynamics noninvasively, right heart catheterization continues to be the gold standard to determine hemodynamic parameters. However, some advocate a future time when hemodynamic parameters will confidently be measured

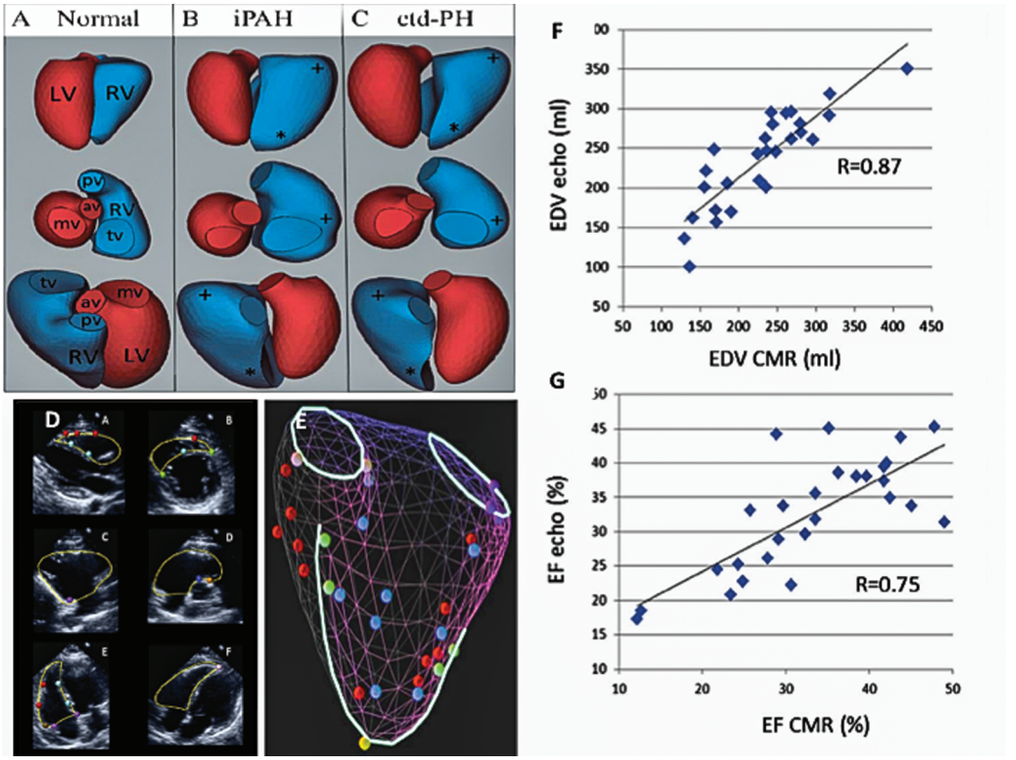

Figure 7. *A–C*, Three-dimensional (3D) reconstructions from patients with a normal heart (*A*), idiopathic pulmonary arterial hypertension (iPAH; *B*), or connective tissue disease related pulmonary hypertension (ctd-PH; *C*), demonstrating apical rounding (asterisks) and basal bulging (plus signs). Adapted from Leary et al.[75] with permission. av: aortic valve; LV: left ventricle; mv: mitral valve; pv: pulmonic valve; RV: right ventricle; tv: tricuspid valve. *D*, Transthoracic echocardiographic images with points placed to define anatomic landmarks and borders of 3D model superimposed (yellow outlines): parasternal long-axis view (*A*), Parasternal short-axis view at the level of the papillary muscles (*B*), RV inflow view (*C*), RV inflow-outflow view (*D*), standard apical 4-chamber view (*E*), and focused RV apical view (*F*). Colors of points are as follows: red for RV endocardium, cyan for interventricular septum, green for RV septal edge, violet for tricuspid annulus, blue for conal septum, orange for pulmonic annulus, brown for basal bulge, and light pink for RV apex. *E*, 3D model of the RV at end-diastole, with endocardial points placed during multiplane initialization. *F*, Bland-Altman analysis comparing TTE-derived measurements with cardiac magnetic resonance imaging (CMR) reference values for end-diastolic volume (EDV). TTE: transthoracic echocardiogram. *G*, Scatterplot analysis comparing TTE-derived measurements with CMR reference values for ejection fraction (EF). *D–G* are adapted from Bhave et al.[79] with permission.

by noninvasive methods, including echocardiography. It remains unclear how current hemodynamics measurements by echocardiography are influencing day-to-day clinical practice.

RV CONTRACTILE RESERVE ASSESSED BY ECHOCARDIOGRAPHY

The concept of using stress, whether during exercise or induced pharmacologically, to evaluate ventricular contractile reserve or the ability to augment function is not new. Most consistently, contractile reserve is evaluated in aortic stenosis and low-flow, low-gradient conditions where the reduced LV systolic function is the focus. However, this framework is analogous in the RV and has been explored in a few disease states, looking at the ability of the RV to improve function as a favorable prognostic sign.[105-108]

Two recent studies have applied the idea of RV reserve to PAH. Blumberg and colleagues[109] took an invasive approach and looked at the ability to increase cardiac index (and thus augmentable RV function) in 26 patients with severe PH from PAH or inoperable chronic thromboembolic pulmonary hypertension. In this study, patients with right ventricle reserve, defined invasively as an increase in RV cardiac index with exercise, had a better prognosis. Grünig and colleagues[110] used a noninvasive approach with Doppler echocardiography to assess RV contractile reserve during exercise, as measured by an increase in pulmonary artery systolic pressure (PASP) of at least 30 mmHg.

Table 3. Commonly used right atrial, right ventricular, and pulmonary pressure estimates by echocardiography

Estimate, formula/method	Concept	Limitations	Sources
1. RAP estimates, normal range of 1–7 mmHg	Elevated RAP is transmitted to the IVC and is visualized by increase in end-expiratory diameter just proximal to junction of hepatic veins and reduced collapse on inspiration		
From IVC diameter and collapsibility: ≤2.1 cm and >50% collapsible = low (<3 mmHg); ≤2.1 cm and <50% collapsible or >2.1 cm and >50% collapsible = intermediate (5–10 mmHg); >2.1 cm and <50% collapsible = high (>15 mmHg)		Not accurate in positive pressure ventilation; less reliable for intermediate pressures values; unknown whether altered by impaired compliance of IVC itself	Brennen et al.;[84] Kircher et al.[87]
Multiple other RA estimates by evaluating systemic veins, hepatic veins, tissue Doppler, and RA size			Review in Beigel et al.[88]
2. RVSP			
Modified Bernoulli equation $4v^2$, where the v is the peak velocity of the TR jet + RAP	Based on the pressure gradient between the right atrium and the right ventricle; first correlated to PASP by Yock and Popp,[91] in the absence of pulmonic stenosis, RVSP can be representative of PASP; in PH screening, PASP > 37 mmHg may indicate need for further invasive measurements	Need TR to estimate pressure; alignment is crucial, maximum TR must be identified from multiple views; subtract gradient across PV if pulmonic stenosis present; avoid arrhythmia; recognition that RVSP elevation may be seen in high-flow states (anemia, high-output high flow) and that the modified Bernoulli equation does not account for abnormal viscosity (as in anemia)	Berger et al.;[13] Currie et al.;[17] Hatle et al.;[89] Skjaerpe and Hatle;[90] Yock and Popp[91]
3. PADP	The end-diastolic pulmonary pressure has been calculated with Bernoulli's formula to the end pulmonic regurgitation pressure + RAP or the RV pressure (based on TR jet) at time of PV opening		

End-diastolic point of the PR jet			Ge et al.;[92] Lee et al.;[93] Ristow et al.[85]
Velocity of the TR jet at time of PV opening			Lanzarini et al.;[94] Reynolds et al.;[95] Stephen et al.[96]
4. mPAP	There are many ways to calculate mPAP from Doppler echocardiography; mPAP currently dictates the severity of PH and has formed the basis of our definition of vasoreactivity	Multiple techniques to establish mPAP	
From PASP: using Doppler-estimated PASP and PADP, mPAP = PADP + (PASP − PADP/3); mPAP = 0.61 (PASP) + 2 mmHg; mPAP = 0.65 (PASP) + 0.55 mmHg; mPAP = 0.6 (PASP)			Chemla et al.;[97] Steckelberg et al.;[98] Syyed et al.[99]
From AcT of the RVOT (also known as PAAT): mPAP = 79 − 0.45 (RVOT AcT) or 90 − 0.62 (RVOT AcT); >100 ms less indicative of PH, <70 ms more indicative of PH			Kitabatake et al.[100]
From tricuspid VTI: mPAP = tricuspid VTI + RAP			Aduen et al.[101]
From PR: 4 × PVR^2 + RAP			Abbas et al.,[102] from work by Masuyama et al.
5. Total pulmonary resistance and PVR			
TR velocity/VTI of RVOT × 10 + 0.16; normal: <1.5 WU (120 dynes × cm/s^2); noninvasive PVR = (RVSP − E/e')/RVOT VTI	Calculation of PVR helps distinguish whether pressure is due to increased flow or from intrinsic pulmonary disease	Not reliable in PVR > 8 WU	Abbas et al.;[86] Dahiya et al.[103]
6. PAC			
SV: LVOT area × LV VTI)/PASP − PADP = SV/ 4 × (TR^2 − PR^2)	Compliance of the pulmonary vasculature is a measure of workload on the RV; change in volume/change in pressure of SV/pulse pressure gives compliance	Reliance on several pressure estimations	Mahapatra et al.[104]

Note: AcT: acceleration time; *E*: tricuspid peak E-wave velocity; *e'*: tricuspid early myocardial velocity; IVC: inferior vena cava; LV: left ventricle; LVOT: left ventricular outflow tract; mPAP: mean pulmonary artery pressure; PAAT: pulmonary artery acceleration time; PAC: pulmonary artery compliance; PADP: pulmonary artery diastolic pressure; PASP: pulmonary artery systolic pressure; PH: pulmonary hypertension; PR: pulmonary regurgitation; PV: pulmonic valve; PVR: pulmonary vascular resistance; RA; right atrial; RAP: right atrial pressure; RV: right ventricular; RVOT: RV outflow tract; RVSP: RV systolic pressure; SV: stroke volume; TR: tricuspid regurgitation; VTI: velocity time integral; WU: Wood units.

Figure 8. Researcher performing echocardiography in an African rural setting.

Patients with the ability to augment PASP had 1-, 3-, and 4-year survival of 96%, 92%, and 89%, respectively, compared to survivals of 92%, 69%, and 48% in patients with low contractile reserve.[110]

INTERNATIONAL ACCESS TO ECHOCARDIOGRAPHY

On the basis of data from the Intersocietal Accreditation Commission, the number of currently accredited adult echocardiography sites in 2013 in the United States is approximately 5,000. However, worldwide access to echocardiography remains limited in most developing countries because of the costs of the technique and the lack of highly specialized personnel to perform it. Echocardiography is portable and safe, uses a simple power supply, and does not require large amounts of maintenance; these characteristics make it the most suitable imaging technique in PAH for low-resource areas, especially those in sub-Saharan Africa. Coincident with this is the fact that more than 200 million people worldwide are infected with schistosomiasis and that approximately 1% of those chronically infected will develop PAH.[111] This is also localized to developing countries, particularly in sub-Saharan Africa. Rheumatic heart disease and endomyocardial fibrosis with subsequent PH are also common in these areas,[112,113] further necessitating the spread of echocardiography into these underserved areas (Fig. 8). Not only will a proliferation of echocardiography in developing countries assist in the diagnosis and characterization of PH, but it will also increase our understanding of these epidemic disease processes and form the basis of imaging and clinical research.[114]

RELEVANCE OF RV IMAGING BY ECHOCARDIOGRAPHY IN CLINICAL DECISION MAKING

The American College of Cardiology/American Heart Association 2009 Expert Consensus Document on Pulmonary Hypertension and the recent Fifth World Symposium on PH recommend basing the initial therapeutic decision for PAH on vasoreactivity testing.[6,115] Subsequent decisions should be based on risk stratification of low- and high-risk PAH patients based on clinical assessment, which may include WHO functional class, physical examination, and/or echocardiography. The recognition of RV dysfunction,

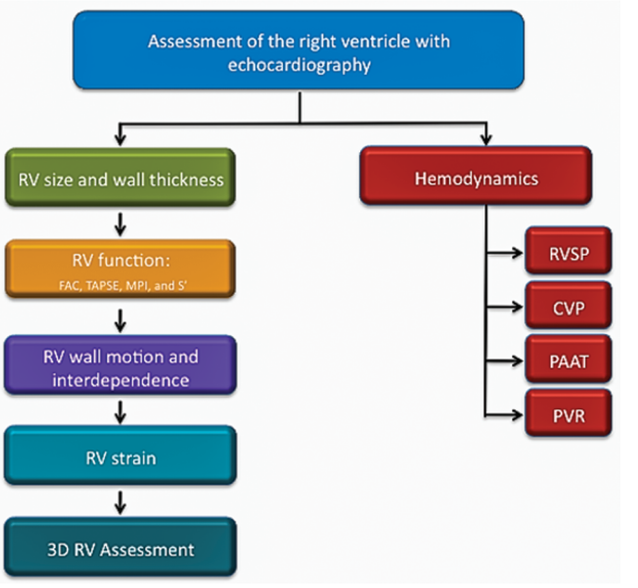

Figure 9. Our approach to RV assessment in echocardiography is summarized. A measurement of size in the apical 4-chamber view evaluating minor and major right ventricular (RV) dimensions is reported, along with RV thickness from the subcostal window. Surrogate measures of RV function routinely evaluated include fractional area change (FAC), tricuspid annulus plane systolic excursion (TAPSE), myocardial performance index (MPI), and systolic velocity (*S'*), with others utilized in research or in times of measurement discrepancies. Comments about qualitative RV wall motion and the relationship between right and left ventricles, as evidenced by septal motion, are described. We highly recommend use of RV strain and three-dimensional (3D) RV assessment in all pulmonary arterial hypertension patients if the capability exists within the clinical setting. Recommended routine noninvasive hemodynamics that can be easily obtained include right ventricular systolic pressure (RVSP), central venous pressure (CVP), pulmonary artery acceleration time (PAAT), and pulmonary vascular resistance (PVR).

RA enlargement, and RV volume overload in PAH leads one to characterize these patients as high-risk, which necessitates consideration of parenteral prostacyclins.[6] With patient outcomes closely tied to the fate of the RV, more knowledge about the effect currently available therapies have on RV dysfunction and investigating new therapies targeting RV dysfunction appears warranted. Our model for a noninvasive evaluation of the RV by echocardiogram is shown in Figure 9.

CONCLUSION

PAH continues to be a very challenging disease to diagnose and manage. Echocardiography has a clear and vital role in both the diagnosis and the management of this disease, and with improved RV imaging, additional ways will become available to evaluate RV structure and function. In particular, 3D echocardiographic imaging of the RV and RV speckle tracking provide accurate and reproducible measures of RV size and function that can be routinely used in clinical practice. In addition, surrogate markers of RV function have been validated against more invasive and extensive assessments of RV performance, such as nuclear ventriculography and cardiac MRI. Continuing advances in acquisition of RV imaging will increase the ability of echocardiography to prognosticate and potentially influence treatment options in PAH. These advances, lower cost, and worldwide availability make echocardiography more attractive as the predominant imaging modality in the longitudinal management of patients with PAH.

ACKNOWLEDGMENTS

We would like to thank Stephen Ishihara, from University of Utah Cardiovascular Imaging Center, for acquisition of images and Kenneth Peake RDCS, from Siemens Cardiovascular Ultrasound, for advice on image processing.

Source of Support: Nil.

Conflict of Interest: None declared.

REFERENCES

1. Farber HW, Loscalzo J. Pulmonary arterial hypertension. New Engl J Med 2004;351(16):1655–1665.
2. Tuder RM, Archer SL, Dorfmüller P, Erzurum SC, Guignabert C, Michelakis E, Rabinovitch M, Schermuly R, Stenmark KR, Morrell NW. Relevant issues in the pathology and pathobiology of pulmonary hypertension. J Am Coll Cardiol 2013;62(25 suppl.):D4–D12.
3. Ling Y, Johnson MK, Kiely DG, Condliffe R, Elliot CA, Gibbs JS, Howard LS, et al. Changing demographics, epidemiology, and survival of incident pulmonary arterial hypertension: results from the pulmonary hypertension registry of the United Kingdom and Ireland. Am J Respir Crit Care Med 2012;186(8):790–796.
4. Humbert M, Sitbon O, Chaouat A, Bertocchi M, Habib G, Gressin V, Yaici A, et al. Pulmonary arterial hypertension in France: results from a national registry. Am J Respir Crit Care Med 2006;173(9):1023–1030.
5. Hoeper MM, Bogaard HJ, Condliffe R, Frantz R, Khanna D, Kurzyna M, Langleben D, et al. Definitions and diagnosis of pulmonary hypertension. J Am Coll Cardiol 2013; 62(25 suppl.):D42–D50.
6. McLaughlin VV, Archer SL, Badesch DB, Barst RJ, Farber HW, Lindner JR, Mathier MA, et al. ACCF/AHA 2009 Expert Consensus Document on pulmonary hypertension: a report of the American College of Cardiology Foundation Task Force on Expert Consensus Documents and the American Heart Association: developed in collaboration with the American College of Chest Physicians, American Thoracic Society, Inc., and the Pulmonary Hypertension Association. Circulation 2009;119(16):2250–2294.
7. Bogaard HJ, Abe K, Vonk Noordegraaf A, Voelkel NF. The right ventricle under pressure: cellular and molecular mechanisms of right-heart failure in pulmonary hypertension. Chest 2009;135(3):794–804.
8. Voelkel NF, Quaife RA, Leinwand LA, Barst RJ, McGoon MD, Meldrum DR, Dupuis J, et al. Right ventricular function and failure: report of a National Heart, Lung, and Blood Institute working group on cellular and molecular mechanisms of right heart failure. Circulation 2006;114(17):1883–1891.
9. Brittain EL, Hemnes AR, Keebler M, Lawson M, Byrd BF III, DiSalvo T. Right ventricular plasticity and functional imaging. Pulm Circ 2012;2(3):309–326.
10. Vonk Noordegraaf A, Galiè N. The role of the right ventricle in pulmonary arterial hypertension. Eur Respir Rev 2011;20 (122):243–253.
11. Chin KM, Kim NH, Rubin LJ. The right ventricle in pulmonary hypertension. Coron Artery Dis 2005;16(1):13–18.
12. Champion HC, Michelakis ED, Hassoun PM. Comprehensive invasive and noninvasive approach to the right ventricle–pulmonary circulation unit: state of the art and clinical and research implications. Circulation 2009;120(11): 992–1007.
13. Berger M, Haimowitz A, Van Tosh A, Berdoff RL, Goldberg E. Quantitative assessment of pulmonary hypertension in patients with tricuspid regurgitation using continuous wave Doppler ultrasound. J Am Coll Cardiol 1985;6 (2):359–365.
14. Denton CP, Cailes JB, Phillips GD, Wells AU, Black CM, Bois RM. Comparison of Doppler echocardiography and right heart catheterization to assess pulmonary hypertension in systemic sclerosis. Br J Rheumatol 1997;36(2): 239–243.
15. Rich JD, Shah SJ, Swamy RS, Kamp A, Rich S. Inaccuracy of Doppler echocardiographic estimates of pulmonary artery pressures in patients with pulmonary hypertension: implications for clinical practice. Chest 2011;139(5):988–993.
16. Janda S, Shahidi N, Gin K, Swiston J. Diagnostic accuracy of echocardiography for pulmonary hypertension: a systematic review and meta-analysis. Heart 2011;97(8):612–622.

17. Currie PJ, Seward JB, Chan KL, Fyfe DA, Hagler DJ, Mair DD, Reeder GS, Nishimura RA, Tajik AJ. Continuous wave Doppler determination of right ventricular pressure: a simultaneous Doppler-catheterization study in 127 patients. J Am Coll Cardiol 1985;6(4):750–756.
18. Piao L, Fang YH, Parikh KS, Ryan JJ, D'Souza KM, Theccanat T, Toth PT, et al. GRK2-mediated inhibition of adrenergic and dopaminergic signaling in right ventricular hypertrophy: therapeutic implications in pulmonary hypertension. Circulation 2012;126(24):2859–2869.
19. Tonelli AR, Arelli V, Minai OA, Newman J, Bair N, Heresi GA, Dweik RA. Causes and circumstances of death in pulmonary arterial hypertension. Am J Respir Crit Care Med 2013;188(3):365–369.
20. Raymond RJ, Hinderliter AL, Willis PW IV, Ralph D, Caldwell EJ, Williams W, Ettinger NA, et al. Echocardiographic predictors of adverse outcomes in primary pulmonary hypertension. J Am Coll Cardiol 2002;39(7):1214–1219.
21. Hinderliter AL, Willis PW IV, Long W, Clarke WR, Ralph D, Caldwell EJ, Williams W, et al. Frequency and prognostic significance of pericardial effusion in primary pulmonary hypertension. Am J Cardiol 1999;84(4):481–484.
22. Eysmann SB, Palevsky HI, Reichek N, Hackney K, Douglas PS. Two-dimensional and Doppler-echocardiographic and cardiac catheterization correlates of survival in primary pulmonary hypertension. Circulation 1989;80(2):353–360.
23. Brierre G, Blot-Souletie N, Degano B, Têtu L, Bongard V, Carrié D. New echocardiographic prognostic factors for mortality in pulmonary arterial hypertension. Eur J Echocardiogr 2010;11(6):516–522.
24. Yeo TC, Dujardin KS, Tei C, Mahoney DW, McGoon MD, Seward JB. Value of a Doppler-derived index combining systolic and diastolic time intervals in predicting outcome in primary pulmonary hypertension. Am J Cardiol 1998; 81(9):1157–1161.
25. Forfia PR, Fisher MR, Mathai SC, Housten-Harris T, Hemnes AR, Borlaug BA, Chamera E, et al. Tricuspid annular displacement predicts survival in pulmonary hypertension. Am J Respir Crit Care Med 2006;174(9):1034–1041.
26. Ghio S, Pazzano AS, Klersy C, Scelsi L, Raineri C, Camporotondo R, D'Armini A, Visconti LO. Clinical and prognostic relevance of echocardiographic evaluation of right ventricular geometry in patients with idiopathic pulmonary arterial hypertension. Am J Cardiol 2011;107(4):628–632.
27. Sachdev A, Villarraga HR, Frantz RP, McGoon MD, Hsiao JF, Maalouf JF, Ammash NM, et al. Right ventricular strain for prediction of survival in patients with pulmonary arterial hypertension. Chest 2011;139(6):1299–1309.
28. Ernande L, Cottin V, Leroux PY, Girerd N, Huez S, Mulliez A, Bergerot C, et al. Right isovolumic contraction velocity predicts survival in pulmonary hypertension. J Am Soc Echocardiogr 2013;26(3):297–306.
29. Ghio S, Gavazzi A, Campana C, Inserra C, Klersy C, Sebastiani R, Arbustini E, Recusani F, Tavazzi L. Independent and additive prognostic value of right ventricular systolic function and pulmonary artery pressure in patients with chronic heart failure. J Am Coll Cardiol 2001;37(1):183–188.
30. Park B, Dittrich HC, Polikar R, Olson L, Nicod P. Echocardiographic evidence of pericardial effusion in severe chronic pulmonary hypertension. Am J Cardiol 1989;63(1): 143–145.
31. Vitarelli A, Terzano C. Do we have two hearts? new insights in right ventricular function supported by myocardial imaging echocardiography. Heart Fail Rev 2010;15:39–61.
32. Harrison A, Wilson BD, Ryan JJ. Exploring the role of aldosterone in right ventricular function. Can J Cardiol 2014; 30(2):155–158.
33. Lang RM, Badano LP, Mor-Avi V, Afilalo J, Armstrong A, Ernande L, Flachskampf FA, et al. Recommendations for cardiac chamber quantification by echocardiography in adults: an update from the American Society of Echocardiography and the European Association of Cardiovascular Imaging. J Am Soc Echocardiogr 2015;28(1):1–39.
34. Jiang L. Right ventricle. In: Weyman AE, ed. Principles and practice of echocardiography. 2nd ed. Baltimore, MD: Lippincott Williams & Wilkins, 1994:901–921.
35. Badano LP, Ginghina C, Easaw J, Muraru D, Grillo MT, Lancellotti P, Pinamonti B, et al. Right ventricle in pulmonary arterial hypertension: haemodynamics, structural changes, imaging, and proposal of a study protocol aimed to assess remodelling and treatment effects. Eur J Echocardiogr 2010; 11(1):27–37.
36. Jiang L, Levine RA, Weyman AE. Echocardiographic assessment of right ventricular volume and function. Echocardiography 1997;14(2):189–206.
37. Sanz J, Conroy J, Narula J. Imaging of the right ventricle. Cardiol Clin 2012;30(2):189–203.
38. Jenkins C, Chan J, Bricknell K, Strudwick M, Marwick TH. Reproducibility of right ventricular volumes and ejection fraction using real-time three-dimensional echocardiography: comparison with cardiac MRI. Chest 2007;131(6): 1844–1851.
39. Ling LF, Obuchowski NA, Rodriguez L, Popovic Z, Kwon D, Marwick TH. Accuracy and interobserver concordance of echocardiographic assessment of right ventricular size and systolic function: a quality control exercise. J Am Soc Echocardiogr 2012;25(7):709–713.
40. Bustamante-Labarta M, Perrone S, De La Fuente RL, Stutzbach P, de la Hoz RP, Torino A, Favaloro R. Right atrial size and tricuspid regurgitation severity predict mortality or transplantation in primary pulmonary hypertension. J Am Soc Echocardiogr 2002;15(10):1160–1164.
41. Matsukubo H, Matsuura T, Endo N, Asayama J, Watanabe T, Furukawa K, Kunishige H, Katsume H, Ijichi H. Echocardiographic measurement of right ventricular wall thickness: a new application of subxiphoid echocardiography. Circulation 1977;56(2):278–284.
42. Ghio S, Klersy C, Magrini G, D'Armini AM, Scelsi L, Raineri C, Pasotti M, Serio A, Campana C, Vigano M. Prognostic relevance of the echocardiographic assessment of right ventricular function in patients with idiopathic pulmonary arterial hypertension. Int J Cardiol 2010;140:272–278.
43. Kawut SM, Barr RG, Lima JA, Praestgaard A, Johnson WC, Chahal H, Ogunyankin KO, et al. Right ventricular structure is associated with the risk of heart failure and cardiovascular death: the Multi-Ethnic Study of Atherosclerosis (MESA)–right ventricle study. Circulation 2012; 126(14):1681–1688.

44. Burke MA, Katz DH, Beussink L, Selvaraj S, Gupta DK, Fox J, Chakrabarti S, et al. Prognostic importance of pathophysiologic markers in patients with heart failure and preserved ejection fraction. Circ Heart Fail 2014;7(2):288–299.
45. Apitz C, Honjo O, Humpl T, Li J, Assad RS, Cho MY, Hong J, Friedberg MK, Redington AN. Biventricular structural and functional responses to aortic constriction in a rabbit model of chronic right ventricular pressure overload. J Thorac Cardiovasc Surg 2012;144(6):1494–1501.
46. Talreja DR, Nishimura RA, Oh JK, Holmes DR. Constrictive pericarditis in the modern era: novel criteria for diagnosis in the cardiac catheterization laboratory. J Am Coll Cardiol 2008;51(3):315–319.
47. Vivo RP, Cordero-Reyes AM, Qamar U, Garikipati S, Trevino AR, Aldeiri M, Loebe M, et al. Increased right-to-left ventricle diameter ratio is a strong predictor of right ventricular failure after left ventricular assist device. J Heart Lung Transplant 2013;32(8):792–799.
48. van de Veerdonk MC, Kind T, Marcus JT, Mauritz GJ, Heymans MW, Bogaard HJ, Boonstra A, Marques KM, Westerhof N, Vonk-Noordegraaf A. Progressive right ventricular dysfunction in patients with pulmonary arterial hypertension responding to therapy. J Am Coll Cardiol 2011;58(24):2511–2519.
49. Schenk P, Globits S, Koller J, Brunner C, Artemiou O, Klepetko W, Burghuber OC. Accuracy of echocardiographic right ventricular parameters in patients with different end-stage lung diseases prior to lung transplantation. J Heart Lung Transplant 2000;19(2):145–154.
50. Anavekar NS, Gerson D, Skali H, Kwong RY, Yucel EK, Solomon SD. Two-dimensional assessment of right ventricular function: an echocardiographic-MRI correlative study. Echocardiography 2007;24(5):452–456.
51. Sengupta PP, Narula J. RV form and function: a piston pump, vortex impeller, or hydraulic ram? JACC Cardiovasc Imaging 2013;6(5):636–639.
52. Hardziyenka M, Campian ME, de Bruin-Bon HA, Michel MC, Tan HL. Sequence of echocardiographic changes during development of right ventricular failure in rat. J Am Soc Echocardiogr 2006;19(10):1272–1279.
53. Tei C, Dujardin KS, Hodge DO, Bailey KR, McGoon MD, Tajik AJ, Seward JB. Doppler echocardiographic index for assessment of global right ventricular function. J Am Soc Echocardiogr 1996;9(6):838–847.
54. Karnati PK, El-Hajjar M, Torosoff M, Fein SA. Myocardial performance index correlates with right ventricular ejection fraction measured by nuclear ventriculography. Echocardiography 2008;25(4):381–385.
55. Lindqvist P, Waldenström A, Henein M, Mörner S, Kazzam E. Regional and global right ventricular function in healthy individuals aged 20–90 years: a pulsed Doppler tissue imaging study: Umeå General Population Heart Study. Echocardiography 2005;22(4):305–314.
56. Meluzín J, Špinarová L, Bakala J, Toman J, Krejčí J, Hude P, Kára T, Souček M. Pulsed Doppler tissue imaging of the velocity of tricuspid annular systolic motion; a new, rapid, and non-invasive method of evaluating right ventricular systolic function. Eur Heart J 2001;22(4):340–348.
57. Gleason WL, Braunwald E. Studies on the first derivative of the ventricular pressure pulse in man. J Clin Invest 1962;41(1):80–91.
58. Imanishi T, Nakatani S, Yamada S, Nakanishi N, Beppu S, Nagata S, Miyatake K. Validation of continuous wave Doppler-determined right ventricular peak positive and negative dP/dt: effect of right atrial pressure on measurement. J Am Coll Cardiol 1994;23(7):1638–1643.
59. Kanzaki H, Nakatani S, Kawada T, Yamagishi M, Sunagawa K, Miyatake K. Right ventricular $dP/dt/P_{max}$, not dP/dt_{max}, noninvasively derived from tricuspid regurgitation velocity is a useful index of right ventricular contractility. J Am Soc Echocardiogr 2002;15(2):136–142.
60. Leather HA, Amà R, Missant C, Rex S, Rademakers FE, Wouters PF. Longitudinal but not circumferential deformation reflects global contractile function in the right ventricle with open pericardium. Am J Physiol Heart Circ Physiol 2006;290(6):H2369–H2375.
61. Reichek N. Right ventricular strain in pulmonary hypertension: flavor du jour or enduring prognostic index? Circ Cardiovasc Imaging 2013;6(5):609–611.
62. Ling LF, Marwick TH. Echocardiographic assessment of right ventricular function: how to account for tricuspid regurgitation and pulmonary hypertension. JACC Cardiovasc Imaging 2012;5(7):747–753.
63. Teske AJ, De Boeck BW, Melman PG, Sieswerda GT, Doevendans PA, Cramer MJ. Echocardiographic quantification of myocardial function using tissue deformation imaging, a guide to image acquisition and analysis using tissue Doppler and speckle tracking. Cardiovasc Ultrasound 2007;5:27. doi:10.1186/1476-7120-5-27.
64. Geyer H, Caracciolo G, Abe H, Wilansky S, Carerj S, Gentile F, Nesser HJ, Khandheria B, Narula J, Sengupta PP. Assessment of myocardial mechanics using speckle tracking echocardiography: fundamentals and clinical applications. J Am Soc Echocardiogr 2010;23(4):351–369, quiz 453–455.
65. Haeck ML, Scherptong RW, Marsan NA, Holman ER, Schalij MJ, Bax JJ, Vliegen HW, Delgado V. Prognostic value of right ventricular longitudinal peak systolic strain in patients with pulmonary hypertension. Circ Cardiovasc Imaging 2012;5(5):628–636.
66. Fine NM, Chen L, Bastiansen PM, Frantz RP, Pellikka PA, Oh JK, Kane GC. Outcome prediction by quantitative right ventricular function assessment in 575 subjects evaluated for pulmonary hypertension. Circ Cardiovasc Imaging 2013;6(5):711–721.
67. Borges AC, Knebel F, Eddicks S, Panda A, Schattke S, Witt C, Baumann G. Right ventricular function assessed by two-dimensional strain and tissue Doppler echocardiography in patients with pulmonary arterial hypertension and effect of vasodilator therapy. Am J Cardiol 2006;98(4):530–534.
68. Hardegree EL, Sachdev A, Villarraga HR, Frantz RP, McGoon MD, Kushwaha SS, Hsiao JF, et al. Role of serial quantitative assessment of right ventricular function by strain in pulmonary arterial hypertension. Am J Cardiol 2013;111(1):143–148.
69. Haddad F, Hunt SA, Rosenthal DN, Murphy DJ. Right ventricular function in cardiovascular disease, part I: anat-

omy, physiology, aging, and functional assessment of the right ventricle. Circulation 2008;117(11):1436–1448.
70. Yang T, Liang Y, Zhang Y, Gu Q, Chen G, Ni XH, Lv XZ, Liu ZH, Xiong CM, He JG. Echocardiographic parameters in patients with pulmonary arterial hypertension: correlations with right ventricular ejection fraction derived from cardiac magnetic resonance and hemodynamics. PLoS ONE 2013;8:e71276. doi:10.1371/journal.pone.0071276.
71. van Wolferen SA, Marcus JT, Boonstra A, Marques KM, Bronzwaer JG, Spreeuwenberg MD, Postmus PE, Vonk-Noordegraaf A. Prognostic value of right ventricular mass, volume, and function in idiopathic pulmonary arterial hypertension. Eur Heart J 2007;28(10):1250–1257.
72. Grapsa J, O'Regan DP, Pavlopoulos H, Durighel G, Dawson D, Nihoyannopoulos P. Right ventricular remodelling in pulmonary arterial hypertension with three-dimensional echocardiography: comparison with cardiac magnetic resonance imaging. Eur J Echocardiogr 2010;11(1):64–73.
73. Lu X, Nadvoretskiy V, Bu L, Stolpen A, Ayres N, Pignatelli RH, Kovalchin JP, Grenier M, Klas B, Ge S. Accuracy and reproducibility of real-time three-dimensional echocardiography for assessment of right ventricular volumes and ejection fraction in children. J Am Soc Echocardiogr 2008;21 (1):84–89.
74. Jiang L, Siu SC, Handschumacher MD, Guererro JL, Vazquez de Prada JA, King ME, Picard MH, Weyman AE, Levine RA. Three-dimensional echocardiography: in vivo validation for right ventricular volume and function. Circulation 1994;89(5):2342–2350.
75. Leary PJ, Kurtz CE, Hough CL, Waiss MP, Ralph DD, Sheehan FH. Three-dimensional analysis of right ventricular shape and function in pulmonary hypertension. Pulm Circ 2012;2(1):34–40.
76. Wong SP, Johnson RK, Sheehan FH. Rapid and accurate left ventricular surface generation from three-dimensional echocardiography by a catalog based method: rapid LV surface generation by three-dimensional echo. Int J Cardiovasc Imaging 2003;19(1):9–17.
77. Hubka M, Bolson EL, McDonald JA, Martin RW, Munt B, Sheehan FH. Three-dimensional echocardiographic measurement of left and right ventricular mass and volume: in vitro validation. Int J Cardiovasc Imaging 2002;18(2):111–118.
78. Kutty S, Li L, Polak A, Gribben P, Danford DA. Echocardiographic knowledge-based reconstruction for quantification of the systemic right ventricle in young adults with repaired d-transposition of great arteries. Am J Cardiol 2012;109(6):881–888.
79. Bhave NM, Patel AR, Weinert L, Yamat M, Freed BH, Mor-Avi V, Gomberg-Maitland M, Lang RM. Three-dimensional modeling of the right ventricle from two-dimensional transthoracic echocardiographic images: utility of knowledge-based reconstruction in pulmonary arterial hypertension. J Am Soc Echocardiogr 2013;26(8):860–867.
80. Milan A, Magnino C, Veglio F. Echocardiographic indexes for the non-invasive evaluation of pulmonary hemodynamics. J Am Soc Echocardiogr 2010;23(3):225–239, quiz 332–334.
81. Howard LS. Prognostic factors in pulmonary arterial hypertension: assessing the course of the disease. Eur Respir Rev 2011;20(122):236–242.
82. Opotowsky AR, Ojeda J, Rogers F, Prasanna V, Clair M, Moko L, Vaidya A, Afilalo J, Forfia PR. A simple echocardiographic prediction rule for hemodynamics in pulmonary hypertension. Circ Cardiovasc Imaging 2012;5(6):765–775.
83. Rudski LG, Lai WW, Afilalo J, Hua L, Handschumacher MD, Chandrasekaran K, Solomon SD, Louie EK, Schiller NB. Guidelines for the echocardiographic assessment of the right heart in adults: a report from the American Society of Echocardiography: endorsed by the European Association of Echocardiography, a registered branch of the European Society of Cardiology, and the Canadian Society of Echocardiography. J Am Soc Echocardiogr 2010;23(7):685–713, quiz 786–788.
84. Brennan JM, Blair JE, Goonewardena S, Ronan A, Shah D, Vasaiwala S, Kirkpatrick JN, Spencer KT. Reappraisal of the use of inferior vena cava for estimating right atrial pressure. J Am Soc Echocardiogr 2007;20(7):857–861.
85. Ristow B, Ahmed S, Wang L, Liu H, Angeja BG, Whooley MA, Schiller NB. Pulmonary regurgitation end-diastolic gradient is a Doppler marker of cardiac status: data from the Heart and Soul Study. J Am Soc Echocardiogr 2005;18 (9):885–891.
86. Abbas AE, Franey LM, Marwick T, Maeder MT, Kaye DM, Vlahos AP, Serra W, Al-Azizi K, Schiller NB, Lester SJ. Noninvasive assessment of pulmonary vascular resistance by Doppler echocardiography. J Am Soc Echocardiogr 2013; 26(10):1170–1177.
87. Kircher BJ, Himelman RB, Schiller NB. Noninvasive estimation of right atrial pressure from the inspiratory collapse of the inferior vena cava. Am J Cardiol 1990;66(4):493–496.
88. Beigel R, Cercek B, Luo H, Siegel RJ. Noninvasive evaluation of right atrial pressure. J Am Soc Echocardiogr 2013; 26(9):1033–1042.
89. Hatle L, Angelsen BA, Tromsdal A. Non-invasive estimation of pulmonary artery systolic pressure with Doppler ultrasound. Br Heart J 1981;45(2):157–165.
90. Skjaerpe T, Hatle L. Noninvasive estimation of systolic pressure in the right ventricle in patients with tricuspid regurgitation. Eur Heart J 1986;7(8):704–710.
91. Yock PG, Popp RL. Noninvasive estimation of right ventricular systolic pressure by Doppler ultrasound in patients with tricuspid regurgitation. Circulation 1984;70(4):657–662.
92. Ge Z, Duran CM, Zhang Y, Ji X, Fan D. Pulmonary artery diastolic pressure: a simultaneous Doppler echocardiography and catheterization study. Clin Cardiol 1992;15(11): 818–824.
93. Lee RT, Lord CP, Plappert T, Sutton MS. Prospective Doppler echocardiographic evaluation of pulmonary artery diastolic pressure in the medical intensive care unit. Am J Cardiol 1989;64(19):1366–1370.
94. Lanzarini L, Fontana A, Lucca E, Campana C, Klersy C. Noninvasive estimation of both systolic and diastolic pulmonary artery pressure from Doppler analysis of tricuspid regurgitant velocity spectrum in patients with chronic heart failure. Am Heart J 2002;144(6):1087–1094.

95. Reynolds DW, Bartelt N, Taepke R, Bennett TD. Measurement of pulmonary artery diastolic pressure from the right ventricle. J Am Coll Cardiol 1995;25(5):1176–1182.
96. Stephen B, Dalal P, Berger M, Schweitzer P, Hecht S. Noninvasive estimation of pulmonary artery diastolic pressure in patients with tricuspid regurgitation by Doppler echocardiography. Chest 1999;116(1):73–77.
97. Chemla D, Castelain V, Humbert M, Hébert JL, Simonneau G, Lecarpentier Y, Hervé P. New formula for predicting mean pulmonary artery pressure using systolic pulmonary artery pressure. Chest 2004;126(4):1313–1317.
98. Steckelberg RC, Tseng AS, Nishimura R, Ommen S, Sorajja P. Derivation of mean pulmonary artery pressure from noninvasive parameters. J Am Soc Echocardiogr 2013;26(5):464–468.
99. Syyed R, Reeves JT, Welsh D, Raeside D, Johnson MK, Peacock AJ. The relationship between the components of pulmonary artery pressure remains constant under all conditions in both health and disease. Chest 2008;133(3):633–639.
100. Kitabatake A, Inoue M, Asao M, Masuyama T, Tanouchi J, Morita T, Mishima M, et al. Noninvasive evaluation of pulmonary hypertension by a pulsed Doppler technique. Circulation 1983;68(2):302–309.
101. Aduen JF, Castello R, Lozano MM, Hepler GN, Keller CA, Alvarez F, Safford RE, Crook JE, Heckman MG, Burger CD. An alternative echocardiographic method to estimate mean pulmonary artery pressure: diagnostic and clinical implications. J Am Soc Echocardiogr 2009;22(7):814–819.
102. Abbas AE, Fortuin FD, Schiller NB, Appleton CP, Moreno CA, Lester SJ. Echocardiographic determination of mean pulmonary artery pressure. Am J Cardiol 2003;92(11):1373–1376.
103. Dahiya A, Vollbon W, Jellis C, Prior D, Wahi S, Marwick T. Echocardiographic assessment of raised pulmonary vascular resistance: application to diagnosis and follow-up of pulmonary hypertension. Heart 2010;96(24):2005–2009.
104. Mahapatra S, Nishimura RA, Oh JK, McGoon MD. The prognostic value of pulmonary vascular capacitance determined by Doppler echocardiography in patients with pulmonary arterial hypertension. J Am Soc Echocardiogr 2006;19(8):1045–1050.
105. Otašević P, Popović Z, Pratali L, Vlahović A, Vasiljević JD, Nešković AN. Right vs. left ventricular contractile reserve in one-year prognosis of patients with idiopathic dilated cardiomyopathy: assessment by dobutamine stress echocardiography. Eur J Echocardiogr 2005;6(6):429–434.
106. Plehn G, Vormbrock J, Perings S, Plehn A, Meissner A, Butz T, Trappe HJ. Comparison of right ventricular functional response to exercise in hypertrophic versus idiopathic dilated cardiomyopathy. Am J Cardiol 2010;105(1):116–121.
107. Matthay RA, Berger HJ, Davies RA, Loke J, Mahler DA, Gottschalk A, Zaret BL. Right and left ventricular exercise performance in chronic obstructive pulmonary disease: radionuclide assessment. Ann Intern Med 1980;93(2):234–239.
108. Vogt M, Kühn A, Wiese J, Eicken A, Hess J, Vogel M. Reduced contractile reserve of the systemic right ventricle under dobutamine stress is associated with increased brain natriuretic peptide levels in patients with complete transposition after atrial repair. Eur J Echocardiogr 2009;10(5):691–694.
109. Blumberg FC, Arzt M, Lange T, Schroll S, Pfeifer M, Wensel R. Impact of right ventricular reserve on exercise capacity and survival in patients with pulmonary hypertension. Eur J Heart Fail 2013;15(7):771–775.
110. Grünig E, Tiede H, Enyimayew EO, Ehlken N, Seyfarth HJ, Bossone E, D'Andrea A, et al. Assessment and prognostic relevance of right ventricular contractile reserve in patients with severe pulmonary hypertension. Circulation 2013;128(18):2005–2015.
111. Graham BB, Bandeira AP, Morrell NW, Butrous G, Tuder RM. Schistosomiasis-associated pulmonary hypertension. Chest 2010;137(6 suppl.):20S–29S.
112. Mocumbi AO, Carrilho C, Sarathchandra P, Ferreira MB, Yacoub M, Burke M. Echocardiography accurately assesses the pathological abnormalities of chronic endomyocardial fibrosis. Int J Cardiovasc Imaging 2011;27(7):955–964.
113. Mocumbi AO, Falase AO. Recent advances in the epidemiology, diagnosis and treatment of endomyocardial fibrosis in Africa. Heart 2013;99(20):1481–1487.
114. Mocumbi AO. Recent trends in the epidemiology of endomyocardial fibrosis in Africa. Paediatr Int Child Health 2012;32(2):63–64.
115. Galiè N, Corris PA, Frost A, Girgis RE, Granton J, Jing ZC, Klepetko W, et al. Updated treatment algorithm of pulmonary arterial hypertension. J Am Coll Cardiol 2013;62(25 suppl.):D60–D72.